A NEW STRATEGY OF DRUG DELIVERY

Student Author

Junxing Shi is a junior undergraduate in biomedical engineering at Purdue University, interested in innovative biotechnologies that can improve our way of living. He had a short-term internship in a national lab in China during the summer of 2013, and he started his own research journey from the Purdue DURI program and *JPUR*. Shi currently is a member of the Center of Implantable Devices (CID) in the Weldon School of Biomedical Engineering at Purdue, working on dielectric properties of artificial materials. He also is a participant of a brain-computer interface project in the Weldon School of Biomedical Engineering.

Mentor

Raji Sundararajan, PhD, is a professor in the Electrical and Computer Engineering Technology Department at Purdue University. She obtained her initial training on electroporation at Johns Hopkins Medical School and spent 8 months at Northwestern Medical School working on electroporation-based gene delivery along with several surgeons. A winner of several awards, Sundararajan also is a reviewer of NIH, NSF (including CAREER awards), US International Science and Technology Center, and US National Research Council proposals. Additionally, she is a reviewer for various scholarly journals, including the *International Journal of Cancer, Molecular Biotechnology,* the *Journal of Biomedical Microdevices,* and the *Journal of Anticancer Drugs, Sensors, and Computers in Biology,* as well as several IEEE transactions.

Abstract

As the second leading cause of cancer-related deaths in children under 20, and the second leading cause of cancer-related deaths in males aged 20–39, there is a need to seek an effective treatment for brain tumors. While there may be various drugs for brain tumors, the problem is the lack of effective methods of delivery through cell membranes at a very specified and confined region. In order to tackle this specific problem of drug delivery, electroporation is introduced. Electroporation, the local application of electrical pulses, renders the cell membranes permeable to otherwise impermeable or poorly permeable anti-cancer drugs, thereby facilitating a potent localized cytotoxic effect. For effective electroporation-based drug uptake, the electric field distribution is critical. If the electric field intensity is too low, it will not open up the pores; if the electric field intensity is too high, it will kill the cells. This study investigated how the applied electric field varied in a 2-D model of a brain slice both with and without tumors, as well as in a simple 3-D model. With a critical field strength at around 1,200 V/cm, simulated electric fields were observed and compared under various conditions. The software utilized was ElecNet, an electric field simulation tool, by which the model was constructed with variable parameters, such as material conductivity and permittivity. Under various conditions, data were collected consistently at relative locations—barely outside, barely inside, and at the center of the tumor—for comparison and analysis. Results in the 2-D model showed the most optimal effect with an 8-needle array electrode, and suggested an enlarged needle array electrode for a large tumor. In 3-D, the critical strength and confined effect were observed at various depths. These results were consistent with previous studies of electroporation on breast tumors, which demonstrated similar electric behaviors. Based on our study, electroporation is a potential therapeutic strategy for treatment of brain tumors. Future investigation of a more sophisticated 3-D model is expected to confirm these findings with other preclinical studies using electroporation.

Shi, J. (2014). A new strategy of drug delivery: Electric field distribution in brain tumor due to electroporation. *Journal of Purdue Undergraduate Research, 4,* 58–65. http://dx.doi.org/10.5703/jpur.04.1.08

Keywords

electroporation, drug delivery, tumor treatment, electric field distribution, computational model, dielectric property, electric-based therapy, finite element model, tumor therapy, brain tumor

http://dx.doi.org/10.5703/jpur.04.1.08

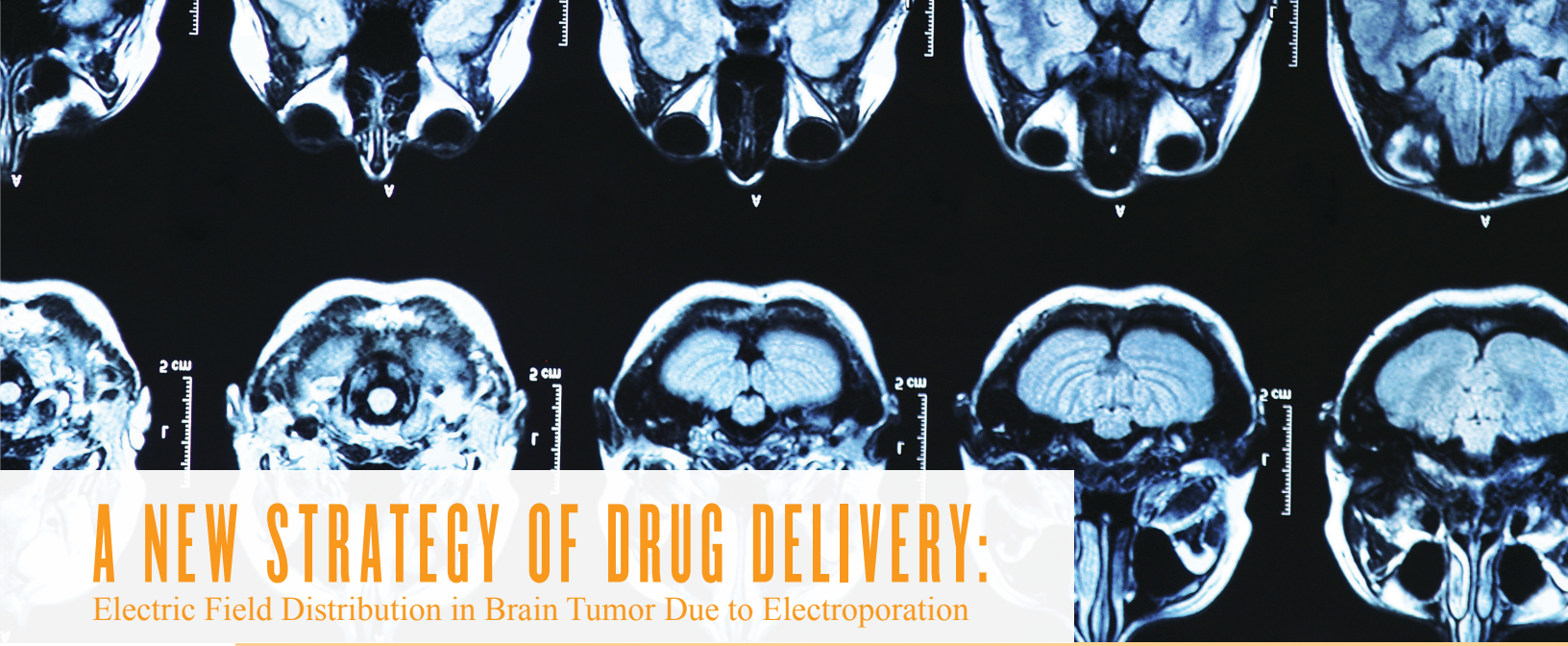

A NEW STRATEGY OF DRUG DELIVERY:

Electric Field Distribution in Brain Tumor Due to Electroporation

Junxing Shi, Biomedical Engineering

INTRODUCTION

Unlike other cancers, brain tumors occur in the most vital and delicate organ of our bodies and are moreover susceptible to all ages, with highly variable and poorly controlled survival rates ranging from 4% to 90%. Brain tumors have thus been the second leading cause of cancer-related deaths in children under 20, and the second leading cause of cancer-related deaths in males aged 20-39 (American Brain Tumor Association, 2014; Ostrom et al., 2013). Therefore, there is a need to find an effective treatment for brain tumors. The standard treatments, consisting of maximal surgical resection, radiotherapy, and chemotherapy, have not yet significantly improved the prognosis of patients with brain tumors. Furthermore, the discovery and development of promising anti-cancer drugs in vitro in the last few decades has not demonstrated any huge impact on the disease in clinical trials. These disappointing results can be explained, if not by the drugs themselves, by the inability of delivering anti-cancer drugs to tumor cells across the blood-brain barrier (BBB), which serves to maintain the brain homeostasis by selectively transporting molecules in and out of the brain. This physiological function of the BBB causes low permeability and poor penetration of anti-cancer drugs to be delivered to the targets, preventing drugs from reaching optimal effects. In addition, with few locally targeting approaches, intake of drugs in natural bio-transport usually led to cytotoxic side effects on surrounding healthy tissues, compromising their treatment effects (Laquintana et al., 2009).

In the hope of resolving the problems of delivery across the BBB, increasing drug penetration, and local tumor targeting, a number of methods have been proposed and studied in recent years (Laquintana et al., 2009). In this paper, a new strategy of drug delivery, termed electroporation, was studied by computational modeling to see the electric field distribution in 2-D and 3-D brain models, and discussed with its positive results against design pitfalls. In an application of such a method, successful treatment of breast cancers in mice using electroporation has been reported (Neal et al., 2010). Electroporation, or electroporation-based therapies and treatments, is a technique used to substantially increase membrane permeability to drugs, which are otherwise poorly transported across tumor membranes. This is achieved by applying preclinically determined electric pulses at critical field strength from 1,000 V/cm to 1,300 V/cm (Čorović, 2013; Neal et al., 2010). It is applied directly on local targeted tumor cells by using minimally invasive electrodes supplied with high voltage pulses, usually in time scale of microseconds. The electric field distribution depends upon the applied voltage magnitude, its duration, and the type of electrodes and the distance between the electrodes (the electrode gap). The high voltage pulses can be applied on a very confined area, reducing cytotoxic side effects on nearby healthy tissues. They also can be applied to reshape the bipolar lipid membrane, and the blood-brain barrier, so that therapeutic drugs can be loaded across otherwise poorly permeable barriers (Čorović, 2013).

Throughout this study, a computer software called ElecNet, which implemented a finite-element algorithm and Maxwell's equations, was used extensively to construct simulation models of the brain on its drawing interface with predetermined dimensional parameters and dielectric properties. It also was used to collect simulation results after its self-processing (ElecNet, 2013). Generated

results were approximated and analyzed to resemble the electrode stimulation during electroporation on brain tumors. Emphasis of variant analyses was made on the 2-D model, while the simple 3-D model was used to demonstrate similar results as in depth.

METHOD

To simulate in ElecNet, the general procedure is to: (1) draw or import a closed bounded object on its drawing interface; (2) assign electrical properties, such as conductivity and permittivity, of the object to be simulated; (3) make electrodes on the object to be stimulated; (4) run simulation with preferable computation options; and (5) collect processed simulation data and results. Our 2-D model of a brain slide was drawn manually as in Figure 1, while the 3-D brain model was imported as a bulk object with fewer features in Figure 2.

2-D Model

To examine the variations on electric field distribution caused by various types of electrodes and sizes of tumor on the 2-D model, two models of a brain slide were drawn as in Figure 1.

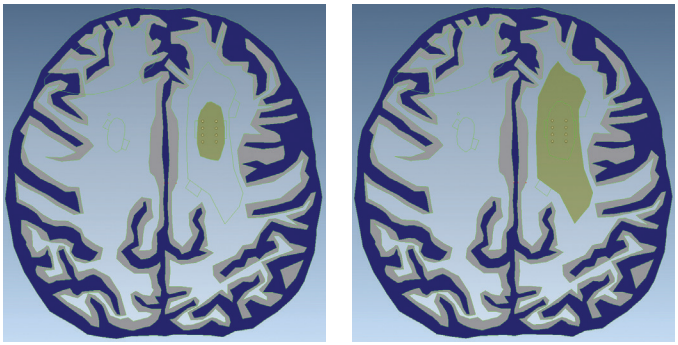

Figure 1. 2-D models of the brain on a scale of 10–15 cm. The left side is a brain slice with a dark gold tumor on a scale of 1–2 cm, while the right side is a brain slice with a dark gold tumor on a scale of 5 cm. Note that both have areas of white matter (light blue color), gray matter (gray color), and meninges layer (dark blue color).

Figure 2. Electrode configurations of plate electrode (left) and needle electrode (right) (Cliniporator Technical Sheet, IGEA, 2010).

On each model, two types of stainless steel 22G electrodes were implemented, respectively, to examine the different electric field distributions. The first type was a plate electrode (Figure 2, left), with a width of 0.1 cm and length of 0.5 cm, mounted directly on two sides of the tumor, horizontally. Based on the distance apart, the voltage supply could be specified accordingly at a critical field strength of around 1,200 V/cm. The second type was an 8-needle array electrode (Figure 2, right), inserted directly in the middle of the tumor, where two lines, spaced by 0.4 cm, of 4 single needles, each spaced by 0.2 cm, lined up with each other. Thus, the voltage supply of the 8-needle electrode was always 480 V.

3-D Model

A simple 3-D model was imported as in Figure 3. Compared to the 2-D model, this model has fewer property features but can be used to examine electric field distribution in depth.

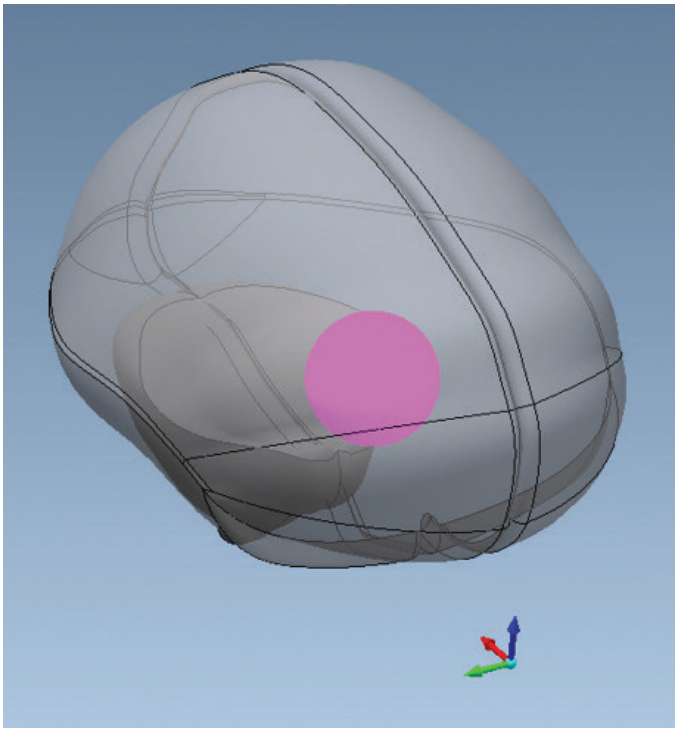

Figure 3. 3-D brain model on a scale of about 15 cm, with a tumor sized 2 cm in radius. Note that only two distinguishable materials are presented in the model.

In this 3-D model, only the 8-needle array electrode was inserted directly into the middle of the tumor. This was because the stimulation effect could easily be seen in depth with a uniform electric field inside, while the plate electrode was difficult to apply on a round surface with much less certainty of electric field distribution underneath the surface and in the target cells.

Parameters

The dielectric properties at 5 kHz, found from the Foundation for Research on Information Technologies in Society (n.d.) were used for simulation. Table 1 provides these values, where nonmeasured values were based on estimation from the best-fit curve (Gabriel, 1996).

Materials used in different models	Conductivity (S/m)	Relative permittivity
Meninges (2-D)	0.5	1.54E3
Tumor (2-D and 3-D)**	260	10.34
White matter (2-D)	0.067	2.09E4
Gray matter (2-D and 3-D) ***	0.11	4.23E4

Table 1. Dielectric properties of simulated materials at 5 kHz.
** Tumor properties were provided based on estimation of breast tumors from our previous work (Agoramurthy & Sundararajan, 2010).
*** Only gray matter was incorporated in the 3-D model, due to: (1) lack of complex structure in this primitive model and (2) the tumor modeled mostly in the cortex is considered primarily gray matter.

Simulation

With the above dielectric properties and position of plate electrodes, 5 kHz pulses with specified voltage supply were simulated in one period of 0.2 milliseconds. Results were displayed at the steady states of maximal electric field distribution with color-shaped gradients, and collected using a built-in electric probe.

RESULTS

Results were shown in two sections. The 2-D section contains four graphs from the four combinations between electrodes and sizes of tumors, and one table and plot for the analysis of electric field strength comparison. The 3-D section contains color gradient graphs from different depths of the tumor.

2-D Simulation

Figures 4–6 illustrate the electric field distributions obtained for the various cases. Figure 4 shows the electric field distributions yielded by the 8-needle array electrode in both the small (left) and the large (right) tumors. They show that the electric field is confined at the optimal strength. Measurement took place along the arrow. Note the inserted electrodes are in gray and that the confined effective region did not cover the entire tumor area. Figure 5 shows the electric field distribution using a plate electrode for the small tumor. Note that the plate electrode is in gray, and the massive covering and invading field toward the healthy region. Measurement took place along the arrow. Figure 6 shows the electric field distribution for plate electrodes on the large tumor. Note the plate electrode is in gray, and the massive covering and invading field toward the healthy region. Measurement took place along the indicated arrow.

Steady state electric field strength was recorded at five relative locations along the indicated arrow in four conditions: (1) left and outside of the tumor boundary; (2) left and inside of the tumor membrane; (3) middle in between the two amounted electrodes along the indicating arrow; (4) right and inside of the tumor membrane; and (5) right and outside

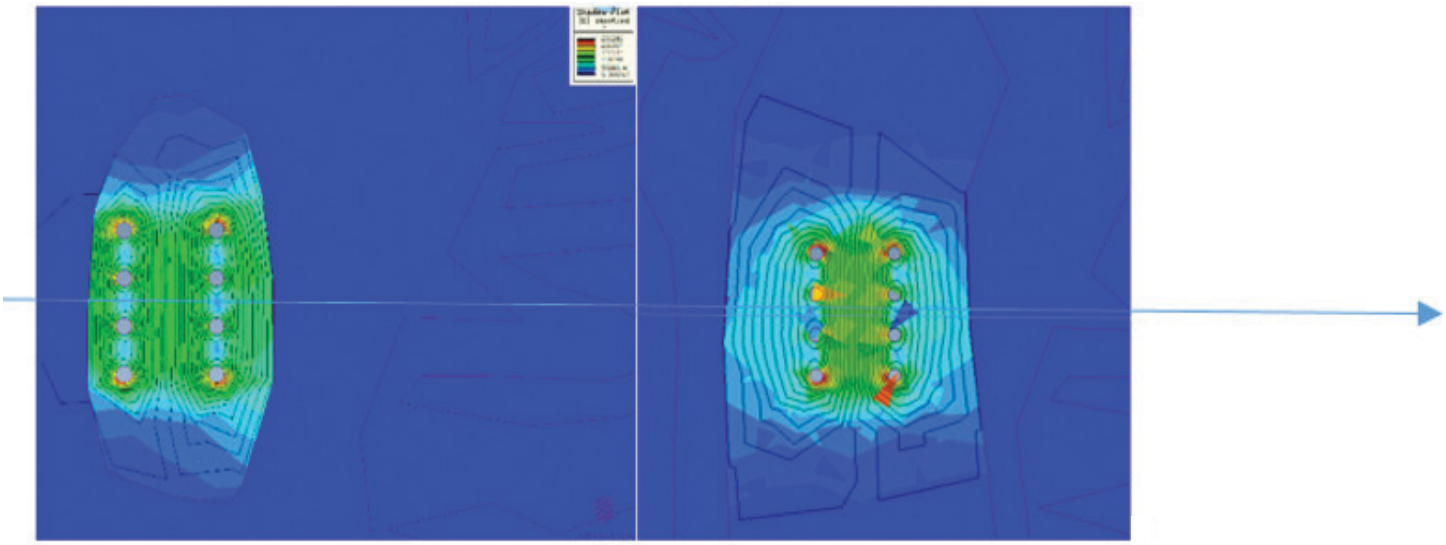

Figure 4. Electric field distributions of the 8-needle electrode in both the small tumor (left) and the large tumor (right) showed confined optimal strength. Measurement took place along the indicated arrow. Note the inserted electrodes in gray and that the confined effective region didn't cover the entire tumor area.

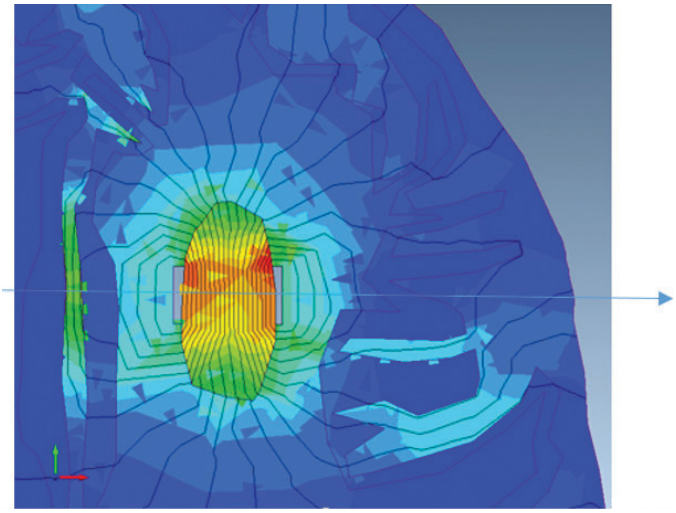

Figure 5. Electric field distribution by plate electrode on small tumor. Note the plate electrode in gray, and the massive covering and invading field toward the healthy region. Measurement took place along the indicated arrow.

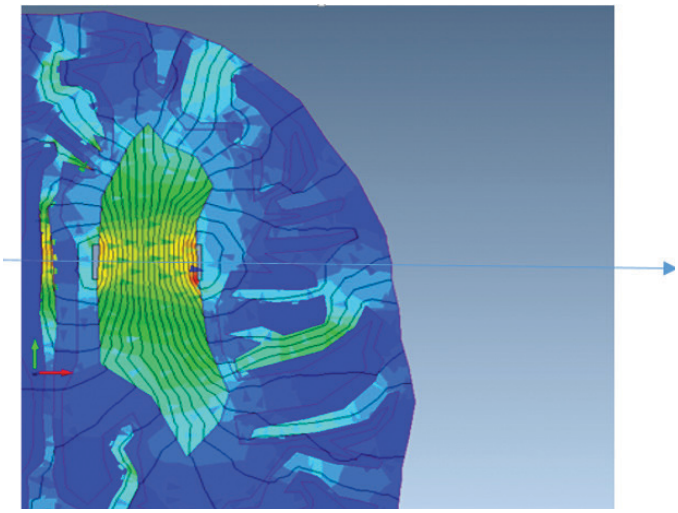

Figure 6. Electric field distribution by plate electrode on the large tumor. Note the plate electrode in gray, and the massive covering and invading field toward the healthy region. Measurement took place along the indicated arrow.

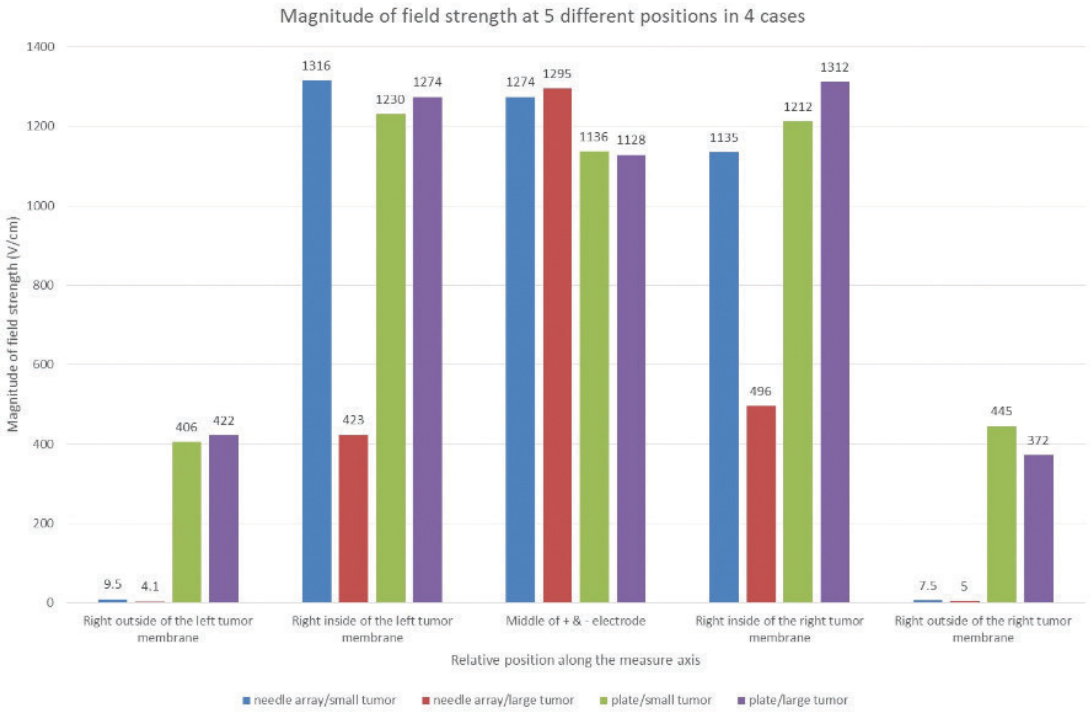

Figure 7. Electric field strengths at four different conditions in five locations. Note the difference in electric field strengths at the same location, but under different conditions.

Relative location	Magnitude of field strength (V/cm)			
	Small + Needle	Large + Needle	Small + Plate	Large + Plate
Left and outside	13	3.8	420	422
Left and inside	1326	462	1279	1290
Middle	1288	1299	1187	1128
Right and inside	1138	599	1254	1316
Right and outside	6.2	4.62	461	362

Table 2. Comparison of Electric field strengths at the five locations.

*Small and large indicate the sizes of tumor, and needle and plate indicate the types of electrodes.

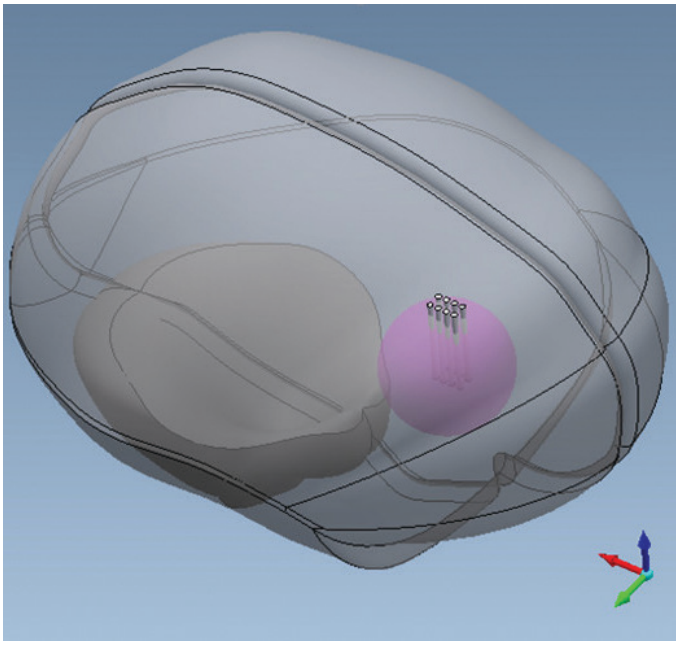

Figure 8. Electrodes inserted into the tumor in 3-D space. Field color maps were extracted from distinct layers from the tumor.

of the tumor membrane. The recorded values were further plotted in bar graphs to emphasize contrast in Figure 7.

3-D Section

Results from the 3-D simulation were demonstrated in 2-D color maps as in the 2-D simulation, but at different depths. Figures 8–11 illustrate the results obtained from the surface of the brain, the surface of the tumor, and the middle of the tumor. Confined optimal field strength was observed in these regions, wherever the needle electrodes were inbound. However, in places where the needles couldn't cover by its own dimension, the field dropped substantially to a minimum.

Figure 8 shows an illustration of the electrodes inserted into the tumor. Field intensities were extracted from distinct layers of the tumor. Figure 9 shows the field distribution on the curved surface of the brain. Here, the field strength gradient increased from 1,000 V/cm to 1,900 V/cm. Figure 10 illustrates the field distribution on the curved surface of the tumor. Here, the strength gradient went from 1,300 V/cm to 1,900 V/cm. Figure 11 shows the field distribution inside of

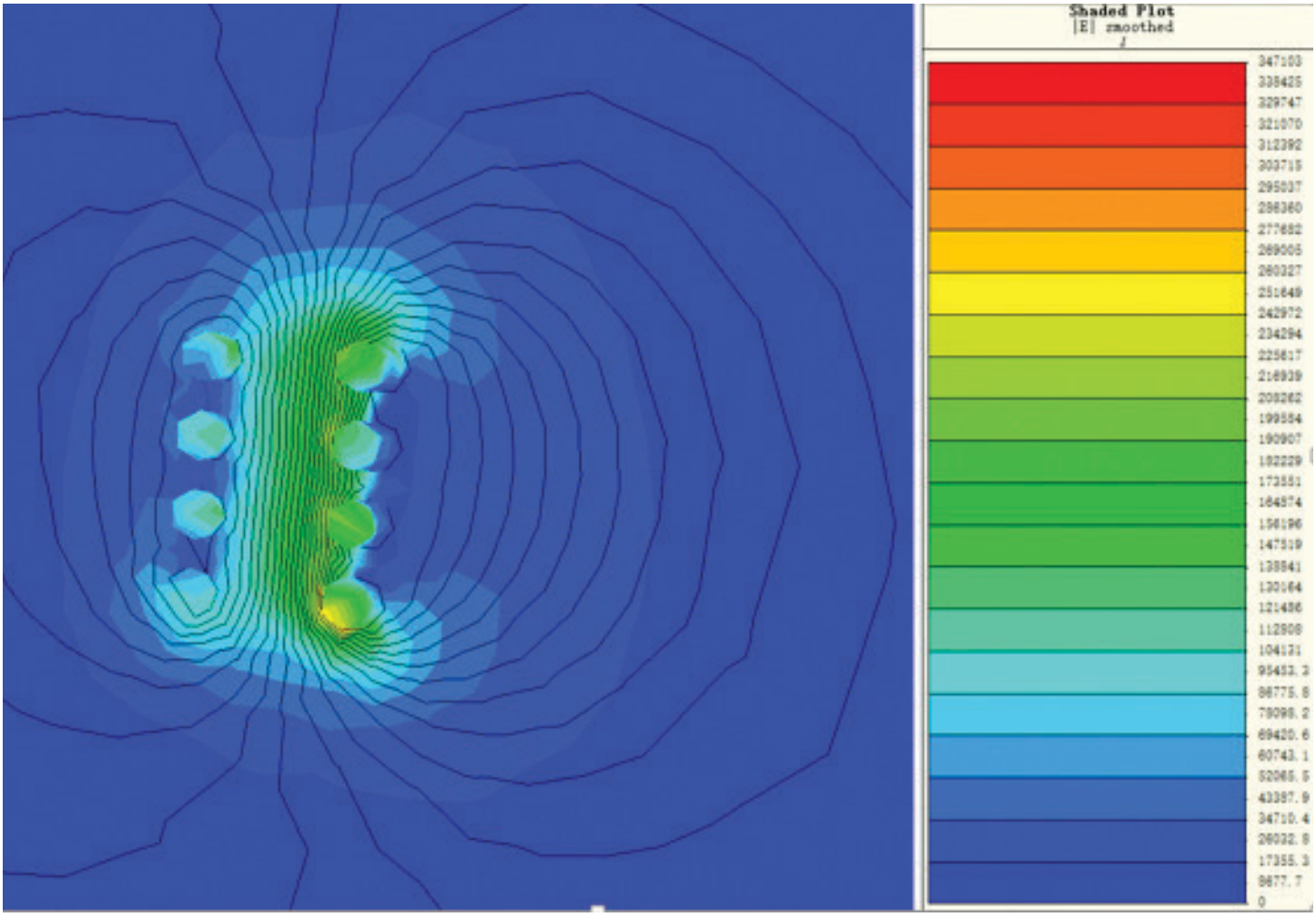

Figure 9. Field distribution on a curved surface of the brain. Note that the strength gradient went from 1,000 V/cm to 1,900 V/cm.

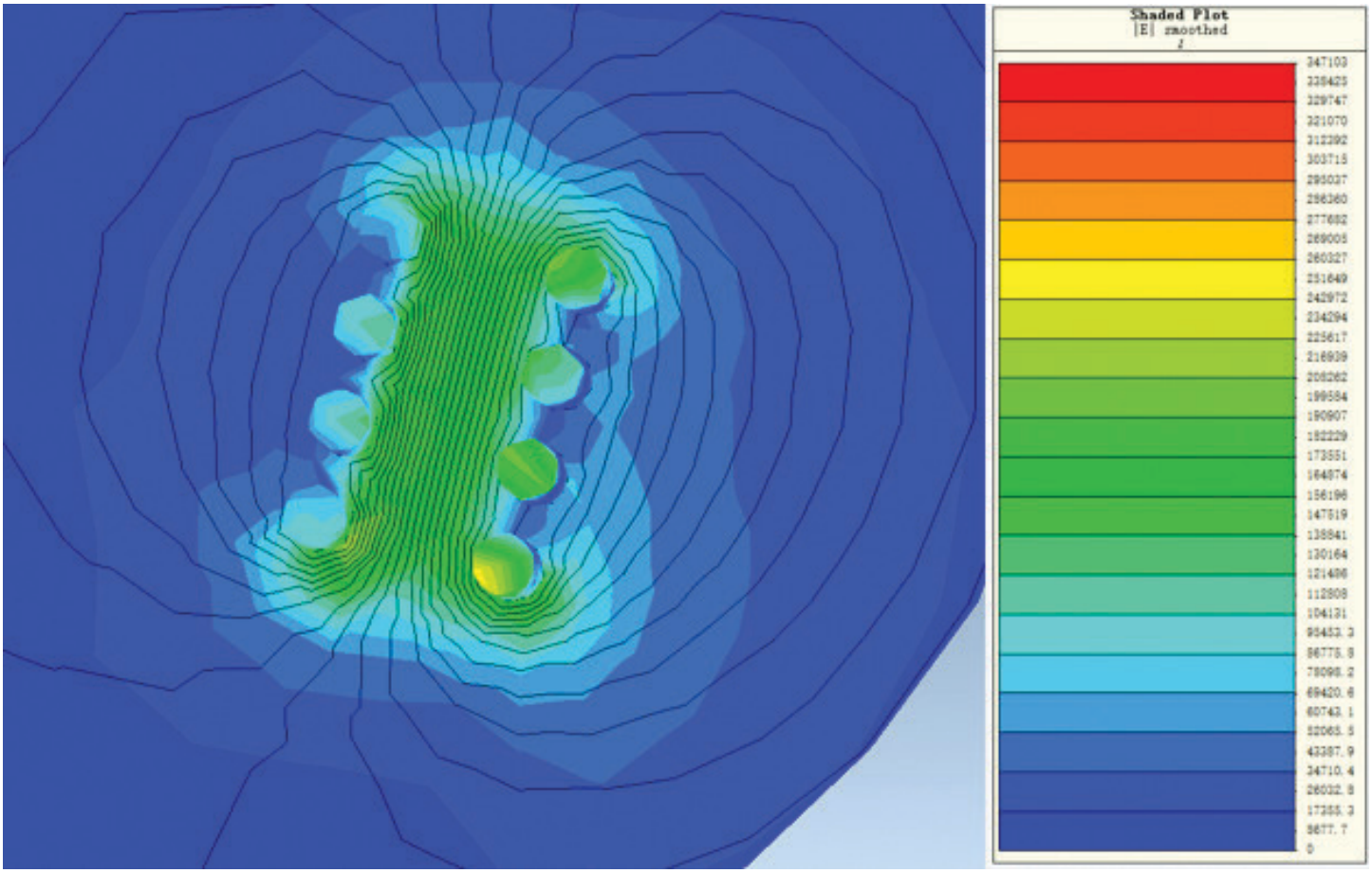

Figure 10. Field distribution on the curved surface of the tumor. Note that the strength gradient went from 1,300 V/cm to 1,900 V/cm.

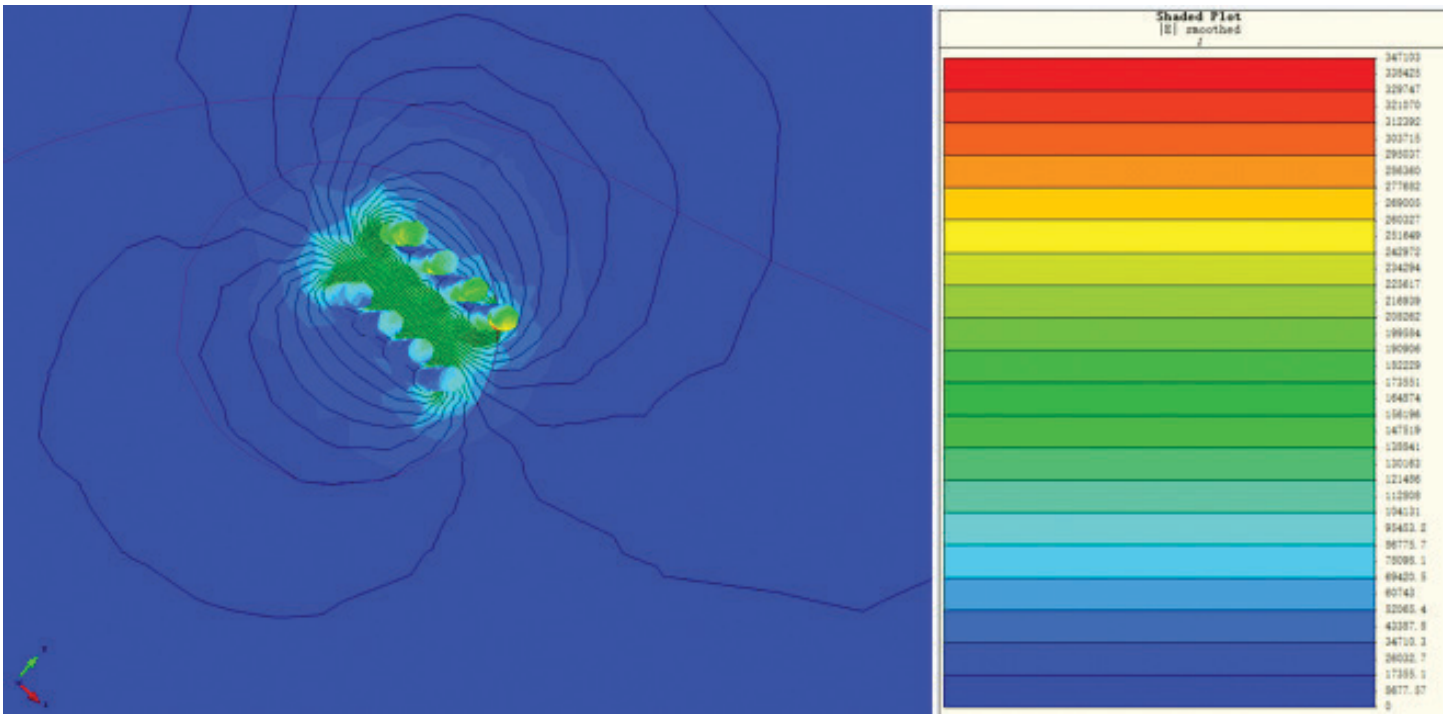

Figure 11. Field distribution inside of the tumor on a flat surface. Note that the field strength was much more uniform at 1,600 V/cm.

the tumor on a flat surface. Here, the field strength was much more uniform at 1,600 V/cm.

Outside of the range of electrode dimensions, field strength in all places dropped to a blue background as the minimum.

CONCLUSIONS

In Figure 4, it was observed that the needle electrode yielded a desirable confined effective region by local simulation, while in Figures 5 and 6, the needle electrode yielded a massive invasion of field into unspecified regions, which was practically unfavorable. According to these simulation results, a targeting therapy using electroporation should take advantage of needle electrodes, rather than plate electrodes, to control localized treatments. This avoids cytotoxic side effects on healthy tissues. This would be extremely important in vital organs, such as human brains, compared to previous studies on breast tumors where researchers utilized plate electrodes (Agoramurthy & Sundararajan, 2010). However, needle electrodes have their pitfalls in not covering the entire region of target, because the local effect was too confined, as seen in Figure 4. A new design of electrode should be considered and proposed to overcome such a problem. Furthermore, in Figure 7, it also has shown numerically that, although all combinations can yield an optimal critical field effect at their maximal strength, there were pitfalls in each single scenario, such that (1) confined effect from the needle electrode failed to cover the entire target area and (2) successful coverage on target areas from the plate electrode came with massive invasion of field toward healthy tissue. Nevertheless, there was one scenario that stood out to be the favorite in the five cases from our simulations. That is, in Figure 4 on the left with a small-sized tumor, the needle electrode stimulated the small tumor and reached critical strength, only covering most of the target area without leakage of energy toward healthy tissues. Based on this particular observation, a hypothesis was proposed to be studied in the future: that a simple, modifiable-in-size needle electrodes can be used for electroporation in tumor target therapy for any size of tumor. However, a potential problem would be if the tumor area was too large, such that the applied needle electrode required a large area of invasion. The study, then, would need to explore multiple ways of stimulations with different electrode designs.

In the 3-D results, more variations were observed during localized stimulation using the needle electrode. The field distribution on a curved surface was no longer uniform as on a flat surface, and even on a flat surface, the computed strength was slightly higher than the desired value. These discrepancies may be attributed to the intrinsic computation, and the different dielectric properties between tumor and normal cells. Nevertheless, it was observed that the field strength became more uniform deep down inside the tumor, and more importantly, the field effective region was confined and bounded by electrode dimension, corresponding to the proposal made from the 2-D results.

Besides these results, there are some limitations and pitfalls in these model structures. Primarily, the model was macroscopic, lacking sophisticated details in many other physiological structures and dielectric features, such as the neuronal transmission by electrical pulses, which occurs massively in the brain. This is common in these types of studies, as all the required details are not available or accessible. In the 3-D model, the structure was intended to demonstrate the local confined field effect in space, including depth; however, the model was too simplified to be considered practical for the same reason.

Future studies on much more refined computational brain model construction are proposed, and the electrical stimulus used in electroporation must be incorporated with neuronal firings in the brain to be considered meaningful and practical as a potential targeting therapy for brain tumors.

ACKNOWLEDGMENTS

I am grateful for the DURI opportunity and thank my faculty mentor, Professor Raji Sundararajan, who educated and inspired me on using such an innovative electric-based approach for tumor treatment. The idea she contributed is very important and invaluable. Further, I want to thank the support team of Infolytica, who provided help and a number of suggestions on using the software analysis tools, and making the 3-D model of the brain. I also appreciate their contribution of the final 3-D brain model for this study.

REFERENCES

Agoramurthy, P., & Sundararajan, R. (2010). Electric field distribution of human breast tissue. *Proceedings from Electrical Insulation and Dielectric Phenomena (CEIDP).* West Lafayette, IN: IEEE. http://dx.doi.org/10.1109/CEIDP.2010.5724064

American Brain Tumor Association. (2014). Brain tumor statistic. Retrieved from http://www.abta.org/about-us/news/brain-tumor-statistics/

Čorović, S., Lacković, I., Šuštaršič, P., Sustar, T., Rodic, T., & Miklavcic, D. (2013). Modeling of electric field distribution in tissues during electroporation. *Biomedical Engineering OnLine, 12,* 1–16. http://dx.doi.org/10.1186/1475-925X-12-16

ElecNet: Predict performance & understand your design: Powerful 2D and 3D electric field simulation software. (2013). Retrieved from http://www.infolytica.com/en/products/elecnet/features.aspx

Foundation for Research on Information Technologies in Society. (n.d.). Database: Dielectric Properties [Data file]. Retrieved from http://www.itis.ethz.ch/itis-for-health/tissue-properties/database/dielectric-properties/

Gabriel, C. (1996). Compilation of the dielectric properties of body tissues at RF and microwave frequencies. Retrieved from http://www.dtic.mil/cgi-bin/GetTRDoc?AD=ADA303903

Laquintana, V., Trapani, A., Denora, N., Wang, F., Gallo, G.M., Tripani, G. (2009). New strategies to deliver anticancer drugs to brain tumors. *Expert Opinion on Drug Delivery, 6*(10), 1017–1032. http://dx.doi.org/10.1517/17425240903167942

Neal, R. E. II, Singh, R., Hatcher, H. C., Kock, N. D., Torti, S. V., & Davalos, R. V. (2010). Treatment of breast cancer through the application of irreversible electroporation using a novel minimally invasive single needle electrode. *Breast Cancer Research and Treatment, 123*(1), 295–301. http://dx.doi.org/10.1007/s10549-010-0803-5

Ostrom, Q. T., Gittleman, H., Farah, P., Ondracek, A., Chen, Y., Wolinsky, Y., . . . Barnholtz-Sloan, J. S. (2013). CBTRUS statistical report: Primary brain and central nervous system tumors diagnosed in the United States in 2006–2010. *Neuro-Oncology, 15*(2), 1–56. http://dx.doi.org/10.1093/neuonc/not151